How to Measure Grana – Ultrastructural Features of Thylakoid Membranes of Plant Chloroplasts

Radosław Mazur[1], Agnieszka Mostowska[2] and Łucja Kowalewska[2]*

[1]*Department of Metabolic Regulation, Institute of Biochemistry, Faculty of Biology, University of Warsaw, Warsaw, Poland,*
[2]*Department of Plant Anatomy and Cytology, Institute of Plant Experimental Biology and Biotechnology, Faculty of Biology, University of Warsaw, Warsaw, Poland*

Granum is a basic structural unit of the thylakoid membrane network of plant chloroplasts. It is composed of multiple flattened membranes forming a stacked arrangement of a cylindrical shape. Grana membranes are composed of lipids and tightly packed pigment-protein complexes whose primary role is the catalysis of photosynthetic light reactions. These membranes are highly dynamic structures capable of adapting to changing environmental conditions by fine-tuning photochemical efficiency, manifested by the structural reorganization of grana stacks. Due to a nanometer length scale of the structural granum features, the application of high-resolution electron microscopic techniques is essential for a detailed analysis of the granum architecture. This mini-review overviews recent approaches to quantitative grana structure analyses from electron microscopy data, highlighting the basic manual measurements and semi-automated workflows. We outline and define structural parameters used by different authors, for instance, granum height and diameter, thylakoid thickness, end-membrane length, Stacking Repeat Distance, and Granum Lateral Irregularity. This article also presents insights into efficient and effective measurements of grana stacks visualized on 2D micrographs. The information on how to correctly interpret obtained data, taking into account the 3D nature of grana stacks projected onto 2D space of electron micrograph, is also given. Grana ultrastructural observations reveal key features of this intriguing membrane arrangement, broadening our knowledge of the thylakoid network's remarkable plasticity.

Keywords: chloroplast, grana, granum stack, measurements, thylakoid membranes, transmission electron microscopy, ultrastructure

GRANA AS BASIC STRUCTURAL UNITS OF THE CHLOROPLAST THYLAKOID NETWORK IN PLANTS

Grana are essential structural features of the chloroplast thylakoid network, which are specific for plants. They are both confined structures characterized by a distinct molecular composition and, simultaneously, continuous elements of intertwined stroma-grana thylakoid network. Other photosynthetic organisms do not have a clear division between stacked grana and loosely arranged stroma thylakoid (ST) domains. Cyanobacteria possess unstacked photosynthetic membranes forming fascicular, radial, or parallel arrangements (Mareš et al., 2019). Similarly,

red algae also do not exhibit thylakoid stacking, while brown algae and diatoms contain appressed membranes grouped by 2 or 3 (Bertrand, 2010). In green algae, the thylakoid membranes are organized into clearly differentiated stacked and unstacked regions but without highly structured multiple membrane layers characteristic for plant grana (Engel et al., 2015). Some authors describe thylakoid membrane stacks of late branching green algae taxa *Coleochaetales* and *Charales* as grana; however, based on the widely accepted evolutionary hypothesis, grana evolved after land colonization and therefore, are unique for plants (Gunning and Schwartz, 1999; Larkum and Vesk, 2003; Mullineaux, 2005). It is worth noticing that although thylakoid membranes of different plant groups, from Bryophytes to Angiosperms, show high variability of photosynthetic complexes supramolecular organization, their grana exhibit similar nano-morphology (Chen et al., 2018b).

From the structural point of view, grana might be described as stacks of discoidal-shaped thylakoids; however, such a general definition is insufficient for detailed qualitative and quantitative analysis of grana structure. A single granum stack is usually composed of 5–25 thylakoid layers with diameters between 300 and 550 nm. The model granum structure is built by thylakoid membranes with the same diameter forming a perfect cylindrical shape. However, in most plant species and specific environmental conditions, the grana structures are highly irregular – with a variable diameter of thylakoid layers and their shift in the lateral plane (**Figure 1A**). It is difficult to structurally distinguish the individual grana stacks with high confidence; therefore, a precise procedure formulation is required (see "**Grana Ultrastructural Parameters**").

General granum definition also does not determine the boundary of the granum in the vertical plane. No limit of the maximal granum height exists; many plant species, especially shade-grown ones, can form grana composed of over 50 layers (Anderson et al., 1973; Chow et al., 2005). Nonetheless, the minimal number of stacked layers that can be considered granum is questionable. The granum stack is built of its core, margins, and end-membranes (**Figure 1B**). These components are characterized by the specific lipid–pigment–protein composition (reviewed in Ruban and Johnson, 2015; Koochak et al., 2019). The boundary of the granum in the lateral plane is set by highly curved membrane regions called grana margins, with peripheries called "curvature domains" that can be biochemically separated (Trotta et al., 2019). Some authors propose a more strict definition of grana margins based on biochemical studies, describing them as an interface between appressed and non-appressed regions only (Rantala et al., 2020). Thylakoids resemble flattened vesicles; they are composed of two membranes and an inner aqueous compartment called "lumen." Neighboring thylakoids in the stack are partitioned by a thin layer of stroma compartment called "stromal gap," "interthylakoid stromal space," or "partition gap" (**Figure 1C**). In the case of core thylakoids, both membranes are identical, while grana end-thylakoids have a heterogeneous architecture; the inner membrane is similar to that of the core thylakoids and the outer one to the ST membrane (Anderson et al., 2012). Considering all this, the lowest granum stack, which contains all types of structural components, has to be built by at least three thylakoid layers. Already in early ultrastructural studies, the two-layer membrane stacks were described as "membrane overlaps" pointing to a different structural assignment of such arrangements (Gunning and Steer, 1975; **Figure 1D**).

An accurate understanding of the granum structure enables the determination of reliable measuring protocols necessary to provide comparable results obtained by different researchers. Detailed analysis of grana structure provides important information about the thylakoid membrane remodeling forced by plant ontogenesis (Kowalewska et al., 2016; Armarego-Marriott et al., 2019; Pipitone et al., 2021), light intensity and quality (Rozak et al., 2002; Yamamoto et al., 2014; Demmig-Adams et al., 2015; Schumann et al., 2017; Flannery et al., 2021), and other environmental factors (Fq et al., 2012; Jiang et al., 2017; Chen et al., 2018a; Zechmann, 2019; Mazur et al., 2020). However, structural analysis indirectly indicates the organization and efficiency of the photosynthetic light reaction machinery (Pribil et al., 2018; Mazur et al., 2019; Wood et al., 2019; Hepworth et al., 2021) and photonic effects in the thylakoid network (Capretti et al., 2019).

Structural grana analysis using mutants with an aberrant composition of thylakoids is particularly helpful in understanding the role of lipid–pigment–protein components in the self-organization of different membrane shapes, such as curved, flat, and stacked regions (Fristedt et al., 2009; Armbruster et al., 2013; Mazur et al., 2019; Bykowski et al., 2021; Gupta et al., 2021; Raven, 2021). A necessary condition, though not sufficient, to define a given chloroplast-localized structure as granum is membrane stacking. The balance between attractive van der Waals forces, repulsive electrostatic and hydrostructural forces was described as crucial for maintaining grana stacking. The abundance, stability, and surface charge of thylakoid membrane components mainly mediate such balance (Puthiyaveetil et al., 2017).

Several thylakoid membrane components have been recognized to play a crucial role in the fine-tuning of grana structure. Numerous studies showed that changes in the ratio of antenna light-harvesting complexes (LHCII) and core proteins of photosystem II (PSII) induce grana size remodeling. Depletion of chloroplast-encoded PSII subunits caused the formation of "super-grana" containing dozens of membranes (Belgio et al., 2015), while lack of Lhcb1 and Lhcb2 antenna proteins resulted in a significant decrease in grana height (Andersson et al., 2003; Anderson et al., 2012; Pietrzykowska et al., 2014; Nicol et al., 2019). Small grana size is also typical for the *chlorina* mutants, characterized by reduced chlorophyll *b* content (e.g., Kim et al., 2009). Tuning of grana structure was also linked with posttranslational modifications of photosynthetic proteins, e.g., increased polyamination of Lhcb, resulting from overexpression of plastidial transglutaminase, caused the formation of extremely high grana stacks (Ioannidis et al., 2009; Ioannidis et al., 2012). In contrast, decreased acetylation of photosynthetic proteins (Arabidopsis *nsi* mutant) induced the formation of lower stacks compared with wild-type plants (Koskela et al., 2018),
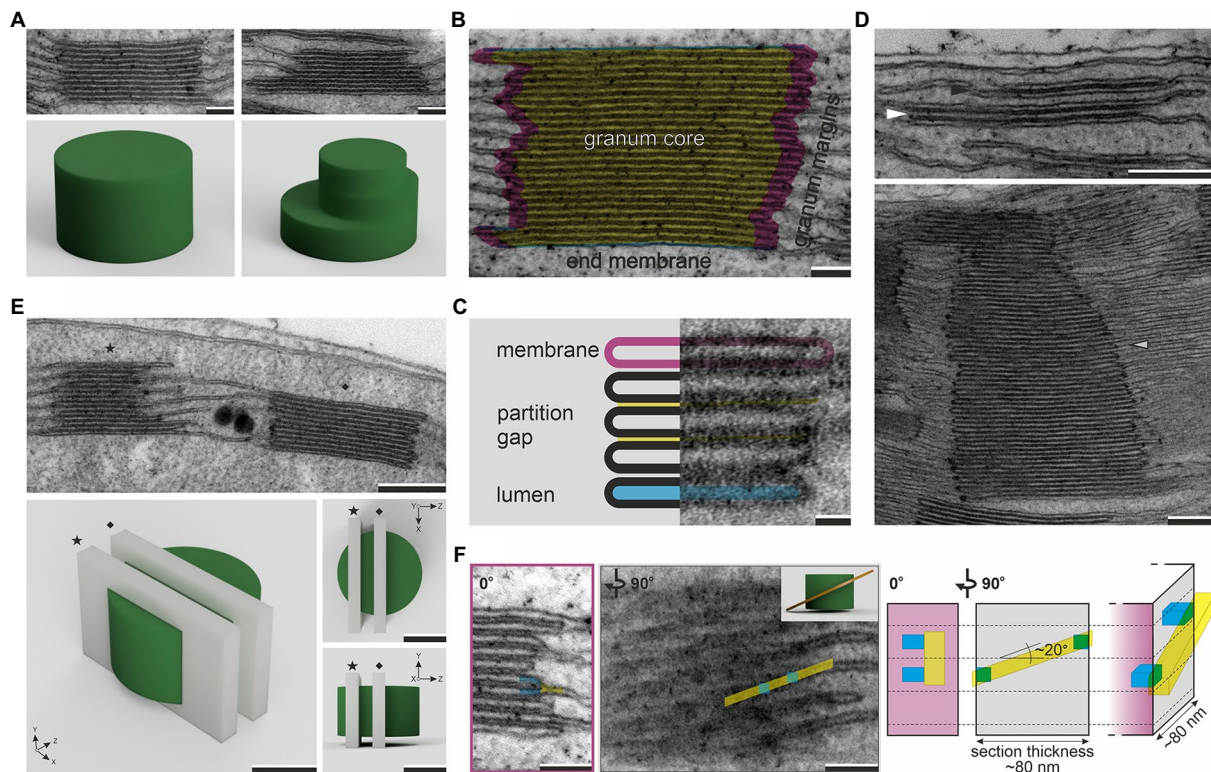
FIGURE 1 | Electron micrographs of regular (left column) and irregular (right column) grana structures with corresponding 3D models showing the hypothetical spatial representation of visualized stacks **(A)**. Three main ultrastructural components of granum stack – granum core (yellow), granum margins (pink), end membranes (blue; **B**). Basic compartments of stacked thylakoids – membrane (pink), partition gap (yellow), and lumen (blue; **C**). Electron micrographs showing two-layer thylakoid membrane stack, i.e., "membrane overlap" (black arrowhead), the lowest possible granum built by three thylakoid layers (white arrowhead), and extremely high granum stack composed of over 70 thylakoid layers (gray arrowhead; **D**). Electron micrograph and corresponding 3D models showing two different z-axis planes (star – tangential cut, diamond – central cut) of random granum sectioning; note that section planes (light gray cuboids) visible on 3D granum renders (green) represent 70-nm-thick ultrathin sections **(E)**. Electron micrographs showing connection of neighboring grana thylakoids through stroma thylakoid (yellow) in the granum marginal region (blue) as visualized from two different angles (inset in the right corner of the second image presents a simplified 3D model of helical grana-stroma thylakoid arrangement); right side of the panel shows a scheme of the connection region visible in the perspective view and two orientations corresponding to presented micrographs; for ultrathin section with thickness between 70 and 90 nm and angle of stroma thylakoid staggering ~20°, connection of two neighboring grana thylakoid layers can be observed in one section and visible as a fork-like structure on the sample projection (transmission electron microscopy (TEM) image; **F**). Note that various angles of granum section showed in panels **(E)** and **(F)** are presented on different grana stacks; electron micrographs were obtained from fully developed chloroplasts of *Arabidopsis thaliana* **(A–F**, with the exception of the lower image in panel **D**) and *Ficus elastica* (lower image on panel **D**); scale bar = 100 nm **(A,B,F)**, 20 nm **(C)**, 250 nm **(D,E)**.

and lack of PSII core protein phosphorylation (Arabidopsis *stn8*, *stn7stn8* mutants) resulted in increased grana diameter (Fristedt et al., 2009).

Moreover, a family of structural membrane proteins – CURVATURE THYLAKOID 1 (CURT1), were recognized to mediate the diameter of grana stacks in a dosage-dependent manner and facilitate membrane curvature at the grana margins (Armbruster et al., 2013; Pribil et al., 2018). The grana-localized REDUCED INDUCTION OF NON-PHOTOCHEMICAL QUENCHING (RIQ) proteins regulate the grana height and probably link the grana structure with the organization of LHCII (Yokoyama et al., 2016). All acyl lipid components of thylakoid membranes were proved to be important in maintaining proper grana sizes; however, only monogalactosyldiacylglycerol role in the formation of helical grana arrangements was shown (Yu and Benning, 2003; Mazur et al., 2019). We have also recently presented that increased

lutein to carotene ratio causing membrane rigidification results in hampered grana membrane folding (Bykowski et al., 2021). In all of these studies, ultrastructural transmission electron microscopy (TEM) analysis was essential to understand structural role of particular membrane components in the grana self-organization process.

METHODS USED IN THE VISUALIZATION OF GRANUM MORPHOLOGY AND THEIR LIMITATIONS

Efficient measurements of grana structural parameters require high-quality visualization of the thylakoid network. The catalog of suitable microscopy methods is limited due to the dimensions

of the grana stacks. In general, these methods can be divided into two groups (i) enabling *in vivo* analysis but with lower resolution, and (ii) high-resolution methods requiring sample fixation.

In vivo methods are mainly based on the detection of chlorophyll autofluorescence (reviewed in Kowalewska et al., 2019). Their advantage lies in the precise tracking of membrane remodeling triggered by different factors. Still, they fail in detailed grana visualization at the level of particular thylakoid layers. Typical grana structural parameters obtained using an *in vivo* approach are granum diameter (Uwada et al., 2017; Wood et al., 2019; Hepworth et al., 2021), also defined as full-width at half-maximum fluorescence intensity of the fluorescent spots (grana; Herbstova et al., 2012; Iwai et al., 2018; Wood et al., 2018; Flannery et al., 2021), and parameters describing the whole network. These parameters include: the number of grana stacks per chloroplast (Wood et al., 2018, 2019; Mazur et al., 2019), their distribution (Herbstova et al., 2012; Chen et al., 2014), and average grana sizes determined indirectly by the surface/volume ratio for 3D models of chlorophyll fluorescence (Bykowski et al., 2021).

High-resolution TEM, although requiring sample fixation, remains the most favored method to study the grana morphology due to the nanometer length scale of the grana structural details. The thylakoid ultrastructure might also be assessed using small-angle scattering methods that enable a noninvasive analysis of high volume samples (Ünnep et al., 2017; Jakubauskas et al., 2019; Ünnep et al., 2020; Zsiros et al., 2020; Jakubauskas et al., 2021). Only periodic membrane attributes can be registered, while no information on grana diameter or details of membrane connections could be revealed. TEM, however, gives access to a broader range of grana structural parameters defined and described in "**Grana Ultrastructural Parameters**" of this mini-review.

Regardless of the numerous advantages of the TEM method in the grana structure studies, particular sample preparation conditions should be considered for a reliable analysis. Due to the relatively small area of TEM analysis, it is essential to control the region of sampling. Chloroplasts of the leaf mesophyll of mono- and dicotyledonous plants do not form a uniform group of organelles. Their thylakoid network is characterized by different structural parameters depending on the leaf age and cell position within the leaf blade (Avramova et al., 2015; Gugel and Soll, 2016). Similarly, a unified time of sample collection is also essential. Suppose sampling throughout the light-dark cycle is not required. In that case, the most favorable time for sample fixation is at the end of the dark phase when the starch grains are, in most cases, degraded, enabling proper observation of the thylakoid network. This approach applies both for samples fixed using chemical and cryo-protocols. High-pressure freezing combined with the freeze-substitution method is particularly susceptible to starch grains whose presence during the procedure leads to the local thylakoid swelling near starch deposits (McDonald, 2014; Armarego-Marriott et al., 2019).

INTERPRETATION OF A 3D GRANA STRUCTURE PROJECTED ONTO 2D SPACE

Although electron microscopy techniques enable a volumetric analysis of samples (electron tomography, serial block-face scanning electron microscopy, or focus ion beam scanning electron microscopy), these techniques are time- and money-consuming. For instance, visualization of the 3D structure of granum using electron tomography requires a multistep procedure composed of data acquisition, alignment, reconstruction, segmentation, and visualization (reviewed in Daum and Kuhlbrandt, 2011; Otegui and Pennington, 2018; Staehelin and Paolillo, 2020). Such extensive workflow limits the possibility of obtaining large data sets and, therefore, reliable quantitative analysis of particular structural parameters. In contrast, 2D TEM analysis is more accessible for researchers and enables the creation of relatively large data sets. However, it is essential to acknowledge that 2D analysis of 3D objects with complicated spatial structures is not straightforward, and the random nature of sample cutting has to be taken into account. The analysis of granum diameter on 2D sections is prone to chord error. It cannot be established whether the observed section shows the diameter or any other chord of the discoidal granum (**Figure 1E**). Therefore, large values of standard deviation are typical for the granum diameter measurements, which points to the necessity of analyzing big data sets for reliable comparison between samples. Another common issue in proper analysis of 2D grana images is related to the interpretation of the structure of grana-stroma thylakoid connections. In these regions, some authors show "fork-like connections" of ST with two neighboring layers of grana stack (fret-like protrusions) using 2D TEM projections (Shimoni et al., 2005; Koochak et al., 2019). However, it should be stressed that such structures are most probably only local phenomena in the *z*-axis of the specimen, which, for 3D models, are parts of STs staggering between granum layers forming pseudo-helical arrangement in the nearest stack surrounding (Mustárdy et al., 2008; Austin and Staehelin, 2011; Kowalewska et al., 2016; Bussi et al., 2019). The typical ultrathin section is 70–90 nm thick; if the granum-connected ST membrane shifts at an angle of around 20° (Austin and Staehelin, 2011; Bussi et al., 2019), membrane staggering between two neighboring layers might be observed within one specimen (for details see **Figure 1F**). TEM images are projections of the visualized sample; therefore, it is impossible to establish the membrane's *z*-axis position inside the sample, and the risk of misinterpretation is significant.

GRANA ULTRASTRUCTURAL PARAMETERS

The first measurements of grana ultrastructural parameters were performed, *in situ*, with the help of mechanical instruments – curvometers on printed electron micrographs of chloroplasts (similarly to measurements on maps). The length of grana
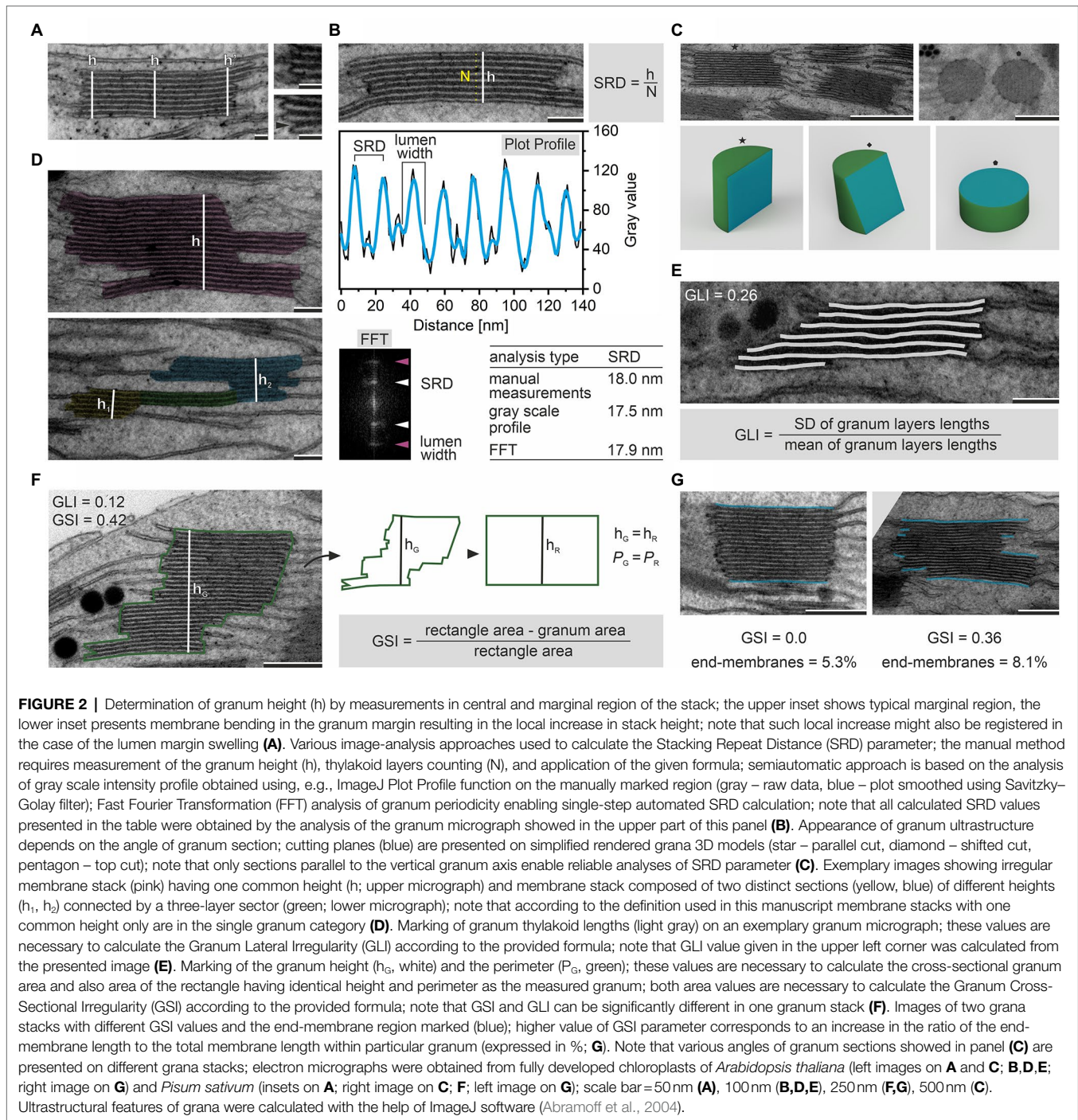
and stroma thylakoids was measured per randomly chosen unit area (1 μm²) of each chloroplast cross section. The number of thylakoids per granum was also determined (e.g., Brangeon, 1973; Mostowska, 1986). Such basic parameters are also frequently assessed in current microscopy studies using digital micrographs and image analysis software of choice, followed by different approaches in data presentation and appropriate statistical analyses (e.g., Rozak et al., 2002; Anderson et al., 2012; Pietrzykowska et al., 2014; Pribil et al., 2018; Wood et al., 2018; Nicol et al., 2019; Li et al., 2020).

Several structural parameters describe the vertical direction of the granum ultrastructure. The most basic one is the granum height. It is established by measuring the distance between the top and bottom layers of the granum end-membranes. Such distance has to be measured perpendicular to the granum lateral plane (Figure 2A). Significant variability in the granum height was registered in plants exposed to different light conditions and connected to the proportion between PSII core and antennae complexes (reviewed in Allen and Forsberg, 2001; Waters and Langdale, 2009; Anderson et al., 2012). The granum height might also be affected by modified physical properties of thylakoid membranes forced by changes in their pigment–protein composition, influencing membrane folding capabilities (Bykowski et al., 2021). Moreover, significant changes in the height of granum stacks were observed in the second phase of the chloroplast biogenesis in different plant species, together with the accumulation of associated photosynthetic proteins and capacity (Armarego-Marriott et al., 2019; Pipitone et al., 2021). In the most general approach, height in the middle of the granum diameter is obtained; however, if the thylakoid thickness is not constant throughout the diameter of the stack, additional measurements have to be taken (for details, see Figure 2A). Such analysis enabled, e.g., observation of swelling and/or bending of the grana marginal regions in plants exposed to high-light conditions to empower more efficient D1 protein turnover (Herbstova et al., 2012; Yoshioka-Nishimura et al., 2014; Kirchhoff, 2019).

Measurement of height combined with the counting of the thylakoid layers that build a particular granum stack enables calculation of the so-called Stacking Repeat Distance (SRD), also named "Repeat Distance," which represents the average thickness of the thylakoid with the neighboring partition gap (Figure 2B). SRD might also be measured directly through manual or semi-automated segmentation of particular granum elements (membrane, lumen, and partition gap) using high magnifications. Various semi-automated approaches based on pixel gradient and power spectrum analyses were applied by different authors (Kirchhoff et al., 2011; Tsabari et al., 2015; Wood et al., 2018; Li et al., 2020; for details, see Figure 2B). It should be noted that all detailed analyses of granum layers require high-quality images of grana stacks cut parallelly to the vertical granum direction (Figure 2C). The analysis of SRD and sizes of particular granum elements is frequently assessed in studies on the influence of light on the thylakoid ion transport resulting in significant changes in, e.g., lumen or partition gap sizes due to water diffusion and changes in repulsive/attractive forces, respectively (Kim et al., 2005; Puthiyaveetil et al., 2017).

The granum lateral (horizontal) plane analysis requires a precise definition of the granum stack boundary. Due to the high variability of grana architecture in the lateral plane, identifying a single granum stack should be justified each time. For instance, it might be assumed that a single granum stack is characterized by (i) common height, which is shared by all stacked membranes building a particular stack, and (ii) shifted regions which are built by at least three stacked membranes (Figure 2D). In such conditions, membrane overlaps connecting neighboring grana are not considered part of these stacks. Therefore, complicated connections of stacked membranes can be quite easily identified for a reliable analysis (Figure 2D). As a consequence of irregular membrane stacks, the granum diameter established in a single measurement of a layer placed in the middle of the granum should be considered as an oversimplification in most cases. Since a granum stack can be built of layers with significantly different diameters (see examples in Figure 1A), a more precise analysis should be provided, where every layer of the granum stack is measured separately, and the average granum diameter is calculated. Calculations of grana diameters were used to understand the connection between the thylakoid structure and the balance between linear and cyclic electron transport (Wood et al., 2018). Diameter measurements were helpful in the establishment of the structural role of CURT1A proteins (Armbruster et al., 2013) and also, e.g., in deciphering the influence of defective PSII core protein phosphorylation on lateral migration of D1 and FtsH proteins between the membrane domains (Khatoon et al., 2009; Puthiyaveetil et al., 2014).

From the diameter values of all membranes building a single granum, a parameter reflecting irregularity of the particular stack called "Granum Lateral Irregularity" (GLI) can be calculated. GLI is defined as the coefficient of variation (the ratio of the standard deviation to the mean) of membrane diameters within the granum (Kowalewska et al., 2016). The minimal GLI value of 0 is reached by grana stacks built of membranes with the same diameter; the higher variability in granum thylakoid diameters, the higher the GLI value (Figure 2E). GLI as a relative variation gives a good measure of irregularity since the chord error of grana thylakoid diameter is minimalized. GLI parameter, however, does not consider the shifting of membranes in the lateral plane. Therefore, we introduce a new parameter that covers this issue giving information about the irregularity of the granum cross section. "Granum Cross-Sectional Irregularity" (GSI) is calculated by comparing the granum cross-sectional area and rectangle area with the same perimeter and height as the granum cross section (Figure 2F). This approach allows identifying irregular grana whose GLI value is close to 0, while membrane shifting in the lateral plane is significant (Figure 2F). Irregular granum arrangement also results in a substantial increase in the ratio of the granum end-membranes to the total stacked membranes; the more irregular granum, the higher the ratio (Figure 2G). Although the height and diameter of grana stacks significantly increase during the initial stages of chloroplast biogenesis, it was established that granum irregularity decreases during this process, indicating an organized structural pathway of grana maturation (Kowalewska et al., 2016). However, the influence of grana structural irregularity on the thylakoid network

FIGURE 2 | Determination of granum height (h) by measurements in central and marginal region of the stack; the upper inset shows typical marginal region, the lower inset presents membrane bending in the granum margin resulting in the local increase in stack height; note that such local increase might also be registered in the case of the lumen margin swelling **(A)**. Various image-analysis approaches used to calculate the Stacking Repeat Distance (SRD) parameter; the manual method requires measurement of the granum height (h), thylakoid layers counting (N), and application of the given formula; semiautomatic approach is based on the analysis of gray scale intensity profile obtained using, e.g., ImageJ Plot Profile function on the manually marked region (gray – raw data, blue – plot smoothed using Savitzky–Golay filter); Fast Fourier Transformation (FFT) analysis of granum periodicity enabling single-step automated SRD calculation; note that all calculated SRD values presented in the table were obtained by the analysis of the granum micrograph showed in the upper part of this panel **(B)**. Appearance of granum ultrastructure depends on the angle of granum section; cutting planes (blue) are presented on simplified rendered grana 3D models (star – parallel cut, diamond – shifted cut, pentagon – top cut); note that only sections parallel to the vertical granum axis enable reliable analyses of SRD parameter **(C)**. Exemplary images showing irregular membrane stack (pink) having one common height (h; upper micrograph) and membrane stack composed of two distinct sections (yellow, blue) of different heights (h_1, h_2) connected by a three-layer sector (green; lower micrograph); note that according to the definition used in this manuscript membrane stacks with one common height only are in the single granum category **(D)**. Marking of granum thylakoid lengths (light gray) on an exemplary granum micrograph; these values are necessary to calculate the Granum Lateral Irregularity (GLI) according to the provided formula; note that GLI value given in the upper left corner was calculated from the presented image **(E)**. Marking of the granum height (h_G, white) and the perimeter (P_G, green); these values are necessary to calculate the cross-sectional granum area and also area of the rectangle having identical height and perimeter as the measured granum; both area values are necessary to calculate the Granum Cross-Sectional Irregularity (GSI) according to the provided formula; note that GSI and GLI can be significantly different in one granum stack **(F)**. Images of two grana stacks with different GSI values and the end-membrane region marked (blue); higher value of GSI parameter corresponds to an increase in the ratio of the end-membrane length to the total membrane length within particular granum (expressed in %; **G**). Note that various angles of granum sections showed in panel **(C)** are presented on different grana stacks; electron micrographs were obtained from fully developed chloroplasts of *Arabidopsis thaliana* (left images on **A** and **C**; **B,D,E**; right image on **G**) and *Pisum sativum* (insets on **A**; right image on **C**; **F**; left image on **G**); scale bar = 50 nm **(A)**, 100 nm **(B,D,E)**, 250 nm **(F,G)**, 500 nm **(C)**. Ultrastructural features of grana were calculated with the help of ImageJ software (Abramoff et al., 2004).

structural reorganization in different conditions is entirely unknown and requires further investigation.

PERSPECTIVES

Although the whole thylakoid network of a single chloroplast forms a continuous arrangement, the grana stacks are structurally isolated units whose architecture, resulting from a plethora of

interactions between membrane components, might be analyzed quantitatively and qualitatively. Recently, a growing number of studies have shown that the grana nano-morphology itself is a significant factor regulating light harvesting and electron transfer (reviewed in Johnson and Wientjes, 2020). For instance, data derived from quantitative analysis of microscopy images were used to simulate plastocyanin diffusion between stacked and unstacked thylakoid domains. It was shown that a specific range of observed grana diameters results from the optimization

of electron transport limited by efficient diffusion of this long-range electron carrier (Hohner et al., 2020). The establishment of a direct role of grana stacks in the efficient performance of photosynthesis has been a subject of many studies, but reasons for the formation of such distinct membrane structures is still under debate (reviewed in Mullineaux, 2005; Anderson et al., 2008; Nevo et al., 2012; Puthiyaveetil et al., 2016; Lambrev and Akhtar, 2019; Moazzami Gudarzi et al., 2021; Müh et al., 2021). An ultrastructure-focused approach adds another dimension to grana function studies, which earlier has been mainly investigated and conceptualized at the level of protein–protein and protein–lipid interactions (reviewed in Johnson and Wientjes, 2020).

In this mini-review, we focused on the use of 2D TEM for quantitative analysis of grana structure. So far, such measurements are mainly executed using manual methods. They are time-consuming and also susceptible to the "human eye" bias, which only partially might be reduced by blinded experiments. The rapid development of machine learning in analyzing different microscopy data (Rawat and Wang, 2017) points to the possibility of applying fully automated protocols for obtaining grana structural parameters. Furthermore, the advantages of the electron microscopy methods *per se* can bring the structural analysis of the thylakoid network to a higher level. Recently developed techniques called jointly "*in situ* liquid cell TEM" could, in the future, enable *in vivo* analysis of the thylakoid network nano-morphology (Pu et al., 2020). On the other hand, a similar goal could be achieved by further developing the 3D structural illumination microscopy method to *in vivo* visualize single layers of grana stacks (Chen et al., 2014). Finally, the advancement in the structural analysis of chloroplast thylakoids should also be extended to the region of STs. Their (i) distinctive role in the light phase of photosynthesis, (ii) complicated and highly organized spatial structure (Bussi et al., 2019), and (iii) possible rearrangements in different genotypes (e.g., Armbruster et al., 2013) point to the importance of detailed structural studies of these thylakoid compartments. However, due to the different architecture of grana and stroma thylakoids, such studies will require the introduction of appropriate structural parameters and new measuring protocols that will consider the complex spatial arrangement of the stroma thylakoids.

AUTHOR CONTRIBUTIONS

FUNDING

ACKNOWLEDGMENTS

REFERENCES

Abramoff, M. D., Magalhães, P. J., and Ram, S. J. (2004). Image processing with ImageJ. *Biophoton. Int.* 11, 36–42.

Allen, J. F., and Forsberg, J. (2001). Molecular recognition in thylakoid structure and function. *Trends Plant Sci.* 6, 317–326. doi: 10.1016/S1360-1385(01)02010-6

Anderson, J. M., Chow, W. S., and De Las, R. J. (2008). Dynamic flexibility in the structure and function of photosystem II in higher plant thylakoid membranes: the grana enigma. *Photosynth. Res.* 98, 575–587. doi: 10.1007/s11120-008-9381-3

Anderson, J. M., Goodchild, D. J., and Boardman, N. K. (1973). Composition of the photosystems and chloroplast structure in extreme shade plants. *Biochim. Biophys. Acta Bioenerg.* 325, 573–585. doi: 10.1016/0005-2728(73)90217-X

Anderson, J. M., Horton, P., Kim, E. H., and Chow, W. S. (2012). Towards elucidation of dynamic structural changes of plant thylakoid architecture. *Philos. Trans. R. Soc. Lond. Ser. B Biol. Sci.* 367, 3515–3524. doi: 10.1098/rstb.2012.0373

Andersson, J., Wentworth, M., Walters, R. G., Howard, C. A., Ruban, A. V., Horton, P., et al. (2003). Absence of the Lhcb1 and Lhcb2 proteins of the light-harvesting complex of photosystem II – effects on photosynthesis, grana stacking and fitness. *Plant J.* 35, 350–361. doi: 10.1046/j.1365-313x.2003.01811.x

Armarego-Marriott, T., Kowalewska, L., Burgos, A., Fischer, A., Thiele, W., Erban, A., et al. (2019). Highly resolved systems biology to dissect the etioplast-to-chloroplast transition in tobacco leaves. *Plant Physiol.* 180, 654–681. doi: 10.1104/pp.18.01432

Armbruster, U., Labs, M., Pribil, M., Viola, S., Xu, W., Scharfenberg, M., et al. (2013). *Arabidopsis* CURVATURE THYLAKOID1 proteins modify THYLAKOID architecture by inducing membrane curvature. *Plant Cell* 25, 2661–2678. doi: 10.1105/tpc.113.113118

Austin, J. R., and Staehelin, L. A. (2011). Three-dimensional architecture of grana and stroma thylakoids of higher plants as determined by electron tomography. *Plant Physiol.* 155, 1601–1611. doi: 10.1104/pp.110.170647

Avramova, V., Sprangers, K., and Beemster, G. (2015). The maize leaf: another perspective on growth regulation. *Trends Plant Sci.* 20, 787–797. doi: 10.1016/j.tplants.2015.09.002

Belgio, E., Ungerer, P., and Ruban, A. V. (2015). Light-harvesting superstructures of green plant chloroplasts lacking photosystems. *Plant Cell Environ.* 38, 2035–2047. doi: 10.1111/pce.12528

Bertrand, M. (2010). Carotenoid biosynthesis in diatoms. *Photosynth. Res.* 106, 89–102. doi: 10.1007/s11120-010-9589-x

Brangeon, J. (1973). Compared ontogeny of the two types of chloroplasts of *Zea mays. J. Microsc.* 16, 233–242.

Bussi, Y., Shimoni, E., Weiner, A., Kapon, R., Charuvi, D., Nevo, R., et al. (2019). Fundamental helical geometry consolidates the plant photosynthetic membrane. *Proc. Natl. Acad. Sci. U. S. A.* 116, 22366–22375. doi: 10.1073/pnas.1905994116

Bykowski, M., Mazur, R., Wójtowicz, J., Suski, S., Garstka, M., Mostowska, A., et al. (2021). Too rigid to fold: carotenoid-dependent decrease in thylakoid fluidity hampers the formation of chloroplast grana. *Plant Physiol.* 185, 210–227. doi: 10.1093/plphys/kiaa009

Capretti, A., Ringsmuth, A. K., van Velzen, J. F., Rosnik, A., Croce, R., and Gregorkiewicz, T. (2019). Nanophotonics of higher-plant photosynthetic membranes. *Light Sci. Appl.* 8:5. doi: 10.1038/s41377-018-0116-8

Chen, Y. E., Su, Y. Q., Mao, H. T., Wu, N., Zhu, F., Yuan, M., et al. (2018b). Terrestrial plants evolve highly assembled photosystem complexes in adaptation to light shifts. *Front. Plant Sci.* 9:1811. doi: 10.3389/fpls.2018.01811

Chen, D., Wang, S., Qi, L., Yin, L., and Deng, X. (2018a). Galactolipid remodeling is involved in drought-induced leaf senescence in maize. *Environ. Exp. Bot.* 150, 57–68. doi: 10.1016/j.envexpbot.2018.02.017

Chen, M.-Y., Zhuo, G.-Y., Chen, K.-C., Wu, P.-C., Hsieh, T.-Y., Liu, T.-M., et al. (2014). Multiphoton imaging to identify grana, stroma thylakoid, and starch inside an intact leaf. *BMC Plant Biol.* 14:175. doi: 10.1186/1471-2229-14-175

Chow, W. S., Kim, E.-H., Horton, P., and Anderson, J. M. (2005). Granal stacking of thylakoid membranes in higher plant chloroplasts: the physicochemical forces at work and the functional consequences that ensue. *Photochem. Photobiol. Sci.* 4, 1081–1090. doi: 10.1039/b507310n

Daum, B., and Kuhlbrandt, W. (2011). Electron tomography of plant thylakoid membranes. *J. Exp. Bot.* 62, 2393–2402. doi: 10.1093/jxb/err034

Demmig-Adams, B., Muller, O., Stewart, J. J., Cohu, C. M., and Adams, W. W. (2015). Chloroplast thylakoid structure in evergreen leaves employing strong thermal energy dissipation. *J. Photochem. Photobiol. B* 152, 357–366. doi: 10.1016/j.jphotobiol.2015.03.014

Engel, B. D., Schaffer, M., Kuhn Cuellar, L., Villa, E., Plitzko, J. M., and Baumeister, W. (2015). Native architecture of the *Chlamydomonas* chloroplast revealed by in situ cryo-electron tomography. *elife* 4:e04889. doi: 10.7554/eLife.04889

Flannery, S. E., Hepworth, C., Wood, W. H. J., Pastorelli, F., Hunter, C. N., Dickman, M. J., et al. (2021). Developmental acclimation of the thylakoid proteome to light intensity in *Arabidopsis. Plant J.* 105, 223–244. doi: 10.1111/tpj.15053

Fq, D. Y. H., Yang, X. F., Chen, S. T., Wang, Y. T., Li, J. K., Shen, Q., et al. (2012). Downregulation of chloroplast RPS1 negatively modulates nuclear heat-responsive expression of HsfA2 and its target genes in *Arabidopsis. PLoS Genet.* 8:e1002669. doi: 10.1371/journal.pgen.1002669

Fristedt, R., Willig, A., Granath, P., Crevecoeur, M., Rochaix, J. D., and Vener, A. V. (2009). Phosphorylation of photosystem II controls functional macroscopic folding of photosynthetic membranes in *Arabidopsis. Plant Cell* 21, 3950–3964. doi: 10.1105/tpc.109.069435

Gugel, I. L., and Soll, J. (2016). Chloroplast differentiation in the growing leaves of *Arabidopsis thaliana. Protoplasma* 254, 1857–1866. doi: 10.1007/s00709-016-1057-9

Gunning, B. E. S., and Schwartz, O. M. (1999). Confocal microscopy of thylakoid autofluorescence in relation to origin of grana and phylogeny in the green algae. *Funct. Plant Biol.* 26, 695–708. doi: 10.1071/PP99076

Gunning, B. E. S., and Steer, M. W. (1975). *Ultrastructure and the Biology of Plant Cell*. London: Edward Arnold.

Gupta, T. K., Klumpe, S., Gries, K., Heinz, S., Wietrzynski, W., Ohnishi, N., et al. (2021). Structural basis for VIPP1 oligomerization and maintenance of thylakoid membrane integrity. *Cell* 184, 3643–3659. doi: 10.1016/j.cell.2021.05.011

Hepworth, C., Wood, W. H. J., Emrich-Mills, T. Z., Proctor, M. S., Casson, S., and Johnson, M. P. (2021). Dynamic thylakoid stacking and state transitions work synergistically to avoid acceptor-side limitation of photosystem I. *Nat. Plants* 7, 87–98. doi: 10.1038/s41477-020-00828-3

Herbstova, M., Tietz, S., Kinzel, C., Turkina, M. V., and Kirchhoff, H. (2012). Architectural switch in plant photosynthetic membranes induced by light stress. *Proc. Natl. Acad. Sci. U. S. A.* 109, 20130–20135. doi: 10.1073/pnas.1214265109

Hohner, R., Pribil, M., Herbstova, M., Lopez, L. S., Kunz, H. H., Li, M., et al. (2020). Plastocyanin is the long-range electron carrier between photosystem II and photosystem I in plants. *Proc. Natl. Acad. Sci. U. S. A.* 117, 15354–15362. doi: 10.1073/pnas.2005832117

Ioannidis, N. E., Lopera, O., Santos, M., Torne, J. M., and Kotzabasis, K. (2012). Role of plastid transglutaminase in LHCII polyamination and thylakoid electron and proton flow. *PLoS One* 7:e41979. doi: 10.1371/journal.pone.0041979

Ioannidis, N. E., Ortigosa, S. M., Veramendi, J., Pinto-Marijuan, M., Fleck, I., Carvajal, P., et al. (2009). Remodeling of tobacco thylakoids by over-expression of maize plastidial transglutaminase. *Biochim. Biophys. Acta* 1787, 1215–1222. doi: 10.1016/j.bbabio.2009.05.014

Iwai, M., Roth, M. S., and Niyogi, K. K. (2018). Subdiffraction-resolution live-cell imaging for visualizing thylakoid membranes. *Plant J.* 96, 233–243. doi: 10.1111/tpj.14021

Jakubauskas, D., Kowalewska, Ł., Sokolova, A. V., Garvey, C. J., Mortensen, K., Jensen, P. E., et al. (2019). Ultrastructural modeling of small angle scattering from photosynthetic membranes. *Sci. Rep.* 9:19405. doi: 10.1038/s41598-019-55423-0

Jakubauskas, D., Mortensen, K., Jensen, P. E., and Kirkensgaard, J. (2021). Small-angle x-ray and neutron scattering on photosynthetic membranes. *Front. Chem.* 9:631370. doi: 10.3389/fchem.2021.631370

Jiang, C., Zu, C., Lu, D., Zheng, Q., Shen, J., Wang, H., et al. (2017). Effect of exogenous selenium supply on photosynthesis, Na+ accumulation and antioxidative capacity of maize (*Zea mays* L.) under salinity stress. *Sci. Rep.* 7:42039. doi: 10.1038/srep42039

Johnson, M. P., and Wientjes, E. (2020). The relevance of dynamic thylakoid organisation to photosynthetic regulation. *Biochim. Biophys. Acta Bioenerg.* 1861:148039. doi: 10.1016/j.bbabio.2019.06.011

Khatoon, M., Inagawa, K., Pospísil, P., Yamashita, A., Yoshioka, M., Lundin, B., et al. (2009). Quality control of photosystem II: thylakoid unstacking is necessary to avoid further damage to the D1 protein and to facilitate D1 degradation under light stress in spinach thylakoids. *J. Biol. Chem.* 284, 25343–25352. doi: 10.1074/jbc.M109.007740

Kim, E. H., Chow, W. S., Horton, P., and Anderson, J. M. (2005). Entropy-assisted stacking of thylakoid membranes. *Biochim. Biophys. Acta* 1708, 187–195. doi: 10.1016/j.bbabio.2005.03.011

Kim, E. H., Li, X. P., Razeghifard, R., Anderson, J. M., Niyogi, K. K., Pogson, B. J., et al. (2009). The multiple roles of light-harvesting chlorophyll a/b-protein complexes define structure and optimize function of *Arabidopsis* chloroplasts: a study using two chlorophyll b-less mutants. *Biochim. Biophys. Acta* 1787, 973–984. doi: 10.1016/j.bbabio.2009.04.009

Kirchhoff, H. (2019). Chloroplast ultrastructure in plants. *New Phytol.* 223, 565–574. doi: 10.1111/nph.15730

Kirchhoff, H., Hall, C., Wood, M., Herbstová, M., Tsabari, O., Nevo, R., et al. (2011). Dynamic control of protein diffusion within the granal thylakoid lumen. *Proc. Natl. Acad. Sci. U. S. A.* 108, 20248–20253. doi: 10.1073/pnas.1104141109

Koochak, H., Puthiyaveetil, S., Mullendore, D. L., Li, M., and Kirchhoff, H. (2019). The structural and functional domains of plant thylakoid membranes. *Plant J.* 97, 412–429. doi: 10.1111/tpj.14127

Koskela, M. M., Brunje, A., Ivanauskaite, A., Grabsztunowicz, M., Lassowskat, I., Neumann, U., et al. (2018). Chloroplast acetyltransferase NSI is required for state transitions in *Arabidopsis thaliana. Plant Cell* 30, 1695–1709. doi: 10.1105/tpc.18.00155

Kowalewska, Ł., Bykowski, M., and Mostowska, A. (2019). Spatial organization of thylakoid network in higher plants. *Bot. Lett.* 166, 326–343. doi: 10.1080/23818107.2019.1619195

Kowalewska, L., Mazur, R., Suski, S., Garstka, M., and Mostowska, A. (2016). Three-dimensional visualization of the tubular-lamellar transformation of the internal plastid membrane network during runner bean chloroplast biogenesis. *Plant Cell* 28, 875–891. doi: 10.1105/tpc.15.01053

Lambrev, P. H., and Akhtar, P. (2019). Macroorganisation and flexibility of thylakoid membranes. *Biochem. J.* 476, 2981–3018. doi: 10.1042/BCJ20190080

Larkum, A. W. D., and Vesk, M. (2003). "Algal plastids: their fine structure and properties," in *Photosynthesis in Algae*. eds. A. W. D. Larkum, S. Douglas and J. A. Raven (Dordrecht: Springer), 11–28.

Li, M., Mukhopadhyay, R., Svoboda, V., Oung, H. M. O., Mullendore, D. L., and Kirchhoff, H. (2020). Measuring the dynamic response of the thylakoid architecture in plant leaves by electron microscopy. *Plant Direct* 4:e00280. doi: 10.1002/pld3.280

Mareš, J., Strunecký, O., Bučinská, L., and Wiedermannová, J. (2019). Evolutionary patterns of thylakoid architecture in cyanobacteria. *Front. Microbiol.* 10:277. doi: 10.3389/fmicb.2019.00277

Mazur, R., Gieczewska, K., Kowalewska, Ł., Kuta, A., Proboszcz, M., Gruszecki, W. I., et al. (2020). Specific composition of lipid phases allows retaining an optimal thylakoid membrane fluidity in plant response to low-temperature treatment. *Front. Plant Sci.* 11:723. doi: 10.3389/fpls.2020.00723

Mazur, R., Mostowska, A., Szach, J., Gieczewska, K., Wojtowicz, J., Bednarska, K., et al. (2019). Galactolipid deficiency disturbs spatial arrangement of the thylakoid network in *Arabidopsis thaliana* plants. *J. Exp. Bot.* 70, 4689–4704. doi: 10.1093/jxb/erz219

McDonald, K. L. (2014). Out with the old and in with the new: rapid specimen preparation procedures for electron microscopy of sectioned biological material. *Protoplasma* 251, 429–448. doi: 10.1007/s00709-013-0575-y

Moazzami Gudarzi, M., Aboutalebi, S. H., and Satalov, A. (2021). Is the debate over grana stacking formation finally solved? *Nat. Plants* 7, 277–278. doi: 10.1038/s41477-021-00880-7

Mostowska, A. (1986). Thylakoid and grana formation during the development of pea chloroplasts, illuminated by white, red, and blue low intensity light. *Protoplasma* 134, 88–94. doi: 10.1007/BF01275706

Müh, F., van Oort, B., Puthiyaveetil, S., and Kirchhoff, H. (2021). Reply to: is the debate over grana stacking formation finally solved? *Nat. Plants* 7, 279–281. doi: 10.1038/s41477-021-00881-6

Mullineaux, C. W. (2005). Function and evolution of grana. *Trends Plant Sci.* 10, 521–525. doi: 10.1016/j.tplants.2005.09.001

Mustárdy, L., Buttle, K., Steinbach, G., and Garab, G. (2008). The three-dimensional network of the thylakoid membranes in plants: quasihelical model of the granum-stroma assembly. *Plant Cell* 20, 2552–2557. doi: 10.1105/tpc.108.059147

Nevo, R., Charuvi, D., Tsabari, O., and Reich, Z. (2012). Composition, architecture and dynamics of the photosynthetic apparatus in higher plants. *Plant J.* 70, 157–176. doi: 10.1111/j.1365-313X.2011.04876.x

Nicol, L., Nawrocki, W. J., and Croce, R. (2019). Disentangling the sites of non-photochemical quenching in vascular plants. *Nat. Plants* 5, 1177–1183. doi: 10.1038/s41477-019-0526-5

Otegui, M. S., and Pennington, J. G. (2018). Electron tomography in plant cell biology. *Microscopy* 68, 69–79. doi: 10.1093/jmicro/dfy133

Pietrzykowska, M., Suorsa, M., Semchonok, D. A., Tikkanen, M., Boekema, E. J., Aro, E. M., et al. (2014). The light-harvesting chlorophyll a/b binding proteins Lhcb1 and Lhcb2 play complementary roles during state transitions in *Arabidopsis*. *Plant Cell* 26, 3646–3660. doi: 10.1105/tpc.114.127373

Pipitone, R., Eicke, S., Pfister, B., Glauser, G., Falconet, D., Uwizeye, C., et al. (2021). A multifaceted analysis reveals two distinct phases of chloroplast biogenesis during de-etiolation in *Arabidopsis*. *elife* 10:e62709. doi: 10.7554/eLife.62709

Pribil, M., Sandoval-Ibáñez, O., Xu, W., Sharma, A., Labs, M., Liu, Q., et al. (2018). Fine-tuning of photosynthesis requires CURVATURE THYLAKOID1-mediated THYLAKOID plasticity. *Plant Physiol.* 176, 2351–2364. doi: 10.1104/pp.17.00863

Pu, S., Gong, C., and Robertson, A. W. (2020). Liquid cell transmission electron microscopy and its applications. *R. Soc. Open Sci.* 7:191204. doi: 10.1098/rsos.191204

Puthiyaveetil, S., Kirchhoff, H., and Höhner, R. (2016). "Structural and functional dynamics of the thylakoid membrane system," in *Chloroplasts: Current Research and Future Trends*. ed. H. Kirchhoff (Poole, UK: Caister Academic Press), 59–88.

Puthiyaveetil, S., Tsabari, O., Lowry, T., Lenhert, S., Lewis, R. R., Reich, Z., et al. (2014). Compartmentalization of the protein repair machinery in photosynthetic membranes. *Proc. Natl. Acad. Sci. U. S. A.* 111, 15839–15844. doi: 10.1073/pnas.1413739111

Puthiyaveetil, S., van Oort, B., and Kirchhoff, H. (2017). Surface charge dynamics in photosynthetic membranes and the structural consequences. *Nat. Plants* 3:17020. doi: 10.1038/nplants.2017.20

Rantala, M., Rantala, S., and Aro, E.-M. (2020). Composition, phosphorylation and dynamic organization of photosynthetic protein complexes in plant thylakoid membrane. *Photochem. Photobiol. Sci.* 19, 604–619. doi: 10.1039/D0PP00025F

Raven, J. A. (2021). Determinants, and implications, of the shape and size of thylakoids and cristae. *J. Plant Physiol.* 257:153342. doi: 10.1016/j.jplph.2020.153342

Rawat, W., and Wang, Z. (2017). Deep convolutional neural networks for image classification: a comprehensive review. *Neural Comput.* 29, 2352–2449. doi: 10.1162/neco_a_00990

Rozak, P. R., Seiser, R. M., Wacholtz, W. F., and Wise, R. R. (2002). Rapid, reversible alterations in spinach thylakoid appression upon changes in light intensity. *Plant Cell Environ.* 25, 421–429. doi: 10.1046/j.0016-8025.2001.00823.x

Ruban, A. V., and Johnson, M. P. (2015). Visualizing the dynamic structure of the plant photosynthetic membrane. *Nat. Plants* 1:15161. doi: 10.1038/nplants.2015.161

Schumann, T., Paul, S., Melzer, M., Dormann, P., and Jahns, P. (2017). Plant growth under natural light conditions provides highly flexible short-term acclimation properties toward high light stress. *Front. Plant Sci.* 8:681. doi: 10.3389/fpls.2017.00681

Shimoni, E., Rav-Hon, O., Ohad, I., Brumfeld, V., and Reich, Z. (2005). Three-dimensional organization of higher-plant chloroplast thylakoid membranes revealed by electron tomography. *Plant Cell* 17, 2580–2586. doi: 10.1105/tpc.105.035030

Staehelin, L. A., and Paolillo, D. J. (2020). A brief history of how microscopic studies led to the elucidation of the 3D architecture and macromolecular organization of higher plant thylakoids. *Photosynth. Res.* 145, 237–258. doi: 10.1007/s11120-020-00782-3

Trotta, A., Bajwa, A. A., Mancini, I., Paakkarinen, V., Pribil, M., and Aro, E. M. (2019). The role of phosphorylation dynamics of CURVATURE THYLAKOID 1B in plant thylakoid membranes. *Plant Physiol.* 181, 1615–1631. doi: 10.1104/pp.19.00942

Tsabari, O., Nevo, R., Meir, S., Carrillo, L. R., Kramer, D. M., and Reich, Z. (2015). Differential effects of ambient or diminished CO_2 and O_2 levels on thylakoid membrane structure in light-stressed plants. *Plant J.* 81, 884–894. doi: 10.1111/tpj.12774

Ünnep, R., Paul, S., Zsiros, O., Kovács, L., Székely, N. K., Steinbach, G., et al. (2020). Thylakoid membrane reorganizations revealed by small-angle neutron scattering of *Monstera deliciosa* leaves associated with non-photochemical quenching. *Open Biol.* 10:200144. doi: 10.1098/rsob.200144

Ünnep, R., Zsiros, O., Hörcsik, Z., Markó, M., Jajoo, A., Kohlbrecher, J., et al. (2017). Low-pH induced reversible reorganizations of chloroplast thylakoid membranes – as revealed by small-angle neutron scattering. *Biochim. Biophys. Acta Bioenerg.* 1858, 360–365. doi: 10.1016/j.bbabio.2017.02.010

Uwada, T., Huang, L.-T., Hee, P.-Y., Usman, A., and Masuhara, H. (2017). Size-dependent optical properties of grana inside chloroplast of plant cells. *J. Phys. Chem. B* 121, 915–922. doi: 10.1021/acs.jpcb.6b10204

Waters, M. T., and Langdale, J. A. (2009). The making of a chloroplast. *EMBO J.* 28, 2861–2873. doi: 10.1038/emboj.2009.264

Wood, W. H. J., Barnett, S. F. H., Flannery, S., Hunter, C. N., and Johnson, M. P. (2019). Dynamic thylakoid stacking is regulated by LHCII phosphorylation but not its interaction with PSI. *Plant Physiol.* 180, 2152–2166. doi: 10.1104/pp.19.00503

Wood, W. H. J., MacGregor-Chatwin, C., Barnett, S. F. H., Mayneord, G. E., Huang, X., Hobbs, J. K., et al. (2018). Dynamic thylakoid stacking regulates the balance between linear and cyclic photosynthetic electron transfer. *Nat. Plants* 4, 116–127. doi: 10.1038/s41477-017-0092-7

Yamamoto, Y., Kai, S., Ohnishi, A., Tsumura, N., Ishikawa, T., Hori, H., et al. (2014). Quality control of PSII: behavior of PSII in the highly crowded grana thylakoids under excessive light. *Plant Cell Physiol.* 55, 1206–1215. doi: 10.1093/pcp/pcu043

Yokoyama, R., Yamamoto, H., Kondo, M., Takeda, S., Ifuku, K., Fukao, Y., et al. (2016). Grana-localized proteins, RIQ1 and RIQ2, affect the organization of light-harvesting complex II and grana stacking in *Arabidopsis*. *Plant Cell* 28, 2261–2275. doi: 10.1105/tpc.16.00296

Yoshioka-Nishimura, M., Nanba, D., Takaki, T., Ohba, C., Tsumura, N., Morita, N., et al. (2014). Quality control of photosystem II: direct imaging of the changes in the thylakoid structure and distribution of FtsH proteases in spinach chloroplasts under light stress. *Plant Cell Physiol.* 55, 1255–1265. doi: 10.1093/pcp/pcu079

Yu, B., and Benning, C. (2003). Anionic lipids are required for chloroplast structure and function in *Arabidopsis*. *Plant J.* 36, 762–770. doi: 10.1046/j.1365-313X.2003.01918.x

Zechmann, B. (2019). Ultrastructure of plastids serves as reliable abiotic and biotic stress marker. *PLoS One* 14:e0214811. doi: 10.1371/journal.pone.0214811

Zsiros, O., Ünnep, R., Nagy, G., Almásy, L., Patai, R., Székely, N. K., et al. (2020). Role of protein-water interface in the stacking interactions of granum thylakoid membranes – as revealed by the effects of hofmeister salts. *Front. Plant Sci.* 11:1257. doi: 10.3389/fpls.2020.01257